BIODIVERSITAS
Volume 27, Number 4, April 2026
Pages: 17

ISSN: 1412-033X
E-ISSN: 2085-4722
https://doi.org/10.13057/biodiv/d270424

Outbreak and host range of *Ceratocystis fimbriata* ITS5 causing a lethal wilt disease on *Lansium domesticum* in South Sumatra, Indonesia

RIKO FIRMANTO[1], AHMAD MUSLIM[2,♥], SUWANDI[2], CHANDRA IRSAN[2], HARMAN HAMIDSON[2], RAHMAT PRATAMA[2], YOSSI APRIAN NURSALIM[3]

[1]Graduate Program of Crop Sciences, Faculty of Agriculture, Universitas Sriwijaya. Jl. Padang Selasa No. 524, Palembang 30139, South Sumatra, Indonesia

[2]Department of Plant Protection, Faculty of Agriculture, Universitas Sriwijaya. Jl. Raya Palembang-Prabumulih Km. 32, Ogan Ilir 30662, South Sumatra, Indonesia. Tel.: +62-711-580059, Fax.: +62-711-580276, ♥email: a_muslim@unsri.ac.id

[3]Graduate Program of Agriculture Sciences, Faculty of Agriculture, Universitas Sriwijaya. Jl. Padang Selasa No. 524, Palembang 30139, South Sumatra, Indonesia

Manuscript received: 4 February 2026. Revision accepted: 15 April 2026.

Abstract. *Firmanto R, Muslim A, Suwandi, Irsan C, Hamidson H, Pratama R, Nursalim YA. 2026. Outbreak and host range of* Ceratocystis fimbriata *ITS5 causing a lethal wilt disease on* Lansium domesticum *in South Sumatra, Indonesia. Biodiversitas 27 (4): d270424. https://doi.org/10.13057/biodiv/d270424*. Lethal wilt disease, first reported on *duku* (*Lansium domesticum*) in 2014, has rapidly expanded from Ogan Komering Ulu to multiple regencies across South Sumatra. By 2021, the epidemic reached Muara Enim, transitioning into an increasingly severe outbreak that threatens local biodiversity. This study aims to evaluate current disease development and severity in Muara Enim and characterize the genetic variation and host range of the associated pathogen. Between 2023 and 2025, we surveyed 24 *L. domesticum* orchards, using plots purposively positioned in high-incidence zones to document the epidemic's maximum virulence. Identification of eight fungal isolates from infected sapwood was performed via morphological observation and multi-gene phylogenetic analysis using Internal Transcribed Spacer (ITS) and β-tubulin markers. Pathogenicity was confirmed by Koch's postulates and host-range testing across diverse plant species. Molecular analysis of these representative isolates confirmed their identity as the ITS5 haplotype of *Ceratocystis fimbriata*, suggesting this haplotype is a key driver of the current outbreak. Results indicated high disease virulence; while regional averages varied, disease incidence reached 100% in the most severely affected orchards (e.g., Ujan Mas Lama) by June 2025. In pathogenicity trials, isolates exhibited aggressive infection patterns, producing significant lesions across all tested hosts; *Parkia speciosa* and *Persea americana* were identified as particularly vulnerable. These results indicate that *C. fimbriata* represents a serious threat to *L. domesticum* orchards and may endanger the long-term persistence of local populations in South Sumatra. To mitigate this impact, urgent management strategies are required, including the immediate removal and destruction of infected trees (sanitation felling), strict pruning hygiene to prevent wound-mediated infection, and careful selection of non-host species in mixed-planting systems.

Keywords: ITS5 haplotype, *Ceratocystis fimbriata*, Meliaceae, molecular phylogeny, Muara Enim

INTRODUCTION

Lansium domesticum Corrêa, commonly known as *duku*, is a cornerstone of the agricultural landscape in South Sumatra, Indonesia, particularly within the Muara Enim District. In this region, land allocated for food crops and horticulture reaches 79.02%, with *duku* serving as a leading commodity (Safety et al. 2024). Beyond its economic value, the *duku* tree holds profound cultural significance; many orchards are ancestral heritages with individual trees exceeding 100 years of age. These trees are typically intercropped with *Durio* sp., *Garcinia mangostana*, and *Mangifera indica*, supporting local livelihoods and ecological stability (Atmojo et al. 2018). Due to their longevity and aesthetic appeal, *duku* trees also offer potential for urban greening and high-value seedling enterprises (Sulistyantara et al. 2024).

However, the sustainability of these orchards is under severe threat from the genus *Ceratocystis*, a group of aggressive xylem-colonizing pathogens known to cause lethal wilt globally (Ahmad et al. 2022). These fungi disrupt water transport by colonizing xylem vessels and bark tissues, leading to rapid canopy decline and mortality (Carluccio et al. 2023). The economic impact of *Ceratocystis* is documented worldwide, affecting various forestry and agroforestry crops (Fernandes et al. 2014; Syazwan et al. 2021). These pathogens are frequently facilitated by wound-creating agents, such as insect vectors and physical damage, which allow for rapid entry into perennial host tissues (Rahayu et al. 2015).

In South Sumatra, the history of this epidemic began between 2014 and 2017 along the Komering River, where widespread mortality of *L. domesticum* reached 100% incidence. The causal agent was identified as *Ceratocystis fimbriata* (Suwandi et al. 2021). Since the initial outbreak in Ogan Komering Ulu, the disease has expanded to numerous regencies. While previous reports noted a low-level presence of the disease in Muara Enim as early as 2017 (Muslim et al. 2022), the latest observations we have conducted from 2023 to 2025 indicate that the situation has escalated into a severe new epidemic. This current outbreak has transitioned from isolated cases into widespread

mortality, often resulting in total orchard loss within four to five months of symptom onset. In these severe cases, infection is often preceded by squirrel feeding wounds and exacerbated by *Hypocryphalus mangiferae* (Eggers, 1928) beetles (Muslim et al. 2025).

Despite the escalating crisis, a critical knowledge gap remains regarding the genetic drivers of this new epidemic in Muara Enim. Previous studies in South Sumatra identified three haplotype groups—ITS5, ITS6z, and ITS7b—associated with *L. domesticum* (Harrington et al. 2014). It is currently unknown whether the intensified outbreaks in Muara Enim involve the emergence of additional ITS haplotypes or are driven by the expansion of the previously dominant ITS5 group. Determining whether this severe epidemic is driven by a single, highly aggressive haplotype is essential for understanding pathogen evolution and developing targeted management strategies. If a lack of genetic diversity is confirmed, it suggests that a specific, highly adapted genotype is responsible for the current devastation.

Consequently, this study was designed to provide a comprehensive temporal update and characterization of the intensified *Ceratocystis* epidemic in the Muara Enim region. While previous studies (e.g., Suwandi et al. 2021; Muslim et al. 2022) established the initial presence and identified the pathogen haplotypes in South Sumatra, the present research builds upon these findings by offering high-resolution spatio-temporal data and an expanded host-range evaluation. The study follows three primary objectives: (i) to assess current geographical distribution and disease severity across *L. domesticum* production centers in Muara Enim District, (ii) to identify ITS genotypes of the causal *C. fimbriata* isolates using ITS and β-tubulin molecular markers, and (iii) to evaluate isolate pathogenicity through expanded host-range trials on diverse agroforestry species. Ultimately, these updates are vital for refining mitigation strategies and ensuring the sustainability of Indonesia's plantation sectors amid evolving disease dynamics.

MATERIALS AND METHODS

Disease distribution survey

Between 2023 and 2025, a severe and extensive outbreak of *Ceratocystis* disease was documented across Muara Enim District, South Sumatra, Indonesia (Figure 1). To characterize this epidemic, disease incidence and intensity were assessed in 24 *Lansium domesticum* (*duku*) orchards distributed across two sub-districts: Ujan Mas and Benakat. In Ujan Mas, surveys were conducted in Ujan Mas Baru, Ujan Mas Lama, Pinang Belarik, and Muara Gula Lama. In Benakat, observations were performed in Rami Pasai, Betung, Padang Bindu, and Pagar Dewa, with three orchards surveyed per village. Within each orchard, 26 to 37 *duku* trees were evaluated to ensure a representative assessment of the disease dynamics. Within each orchard, an observational survey was conducted using five 10 × 10 m plots. To maintain temporal consistency across the study period, these surveys were carried out in June 2023, July 2024, and June 2025.

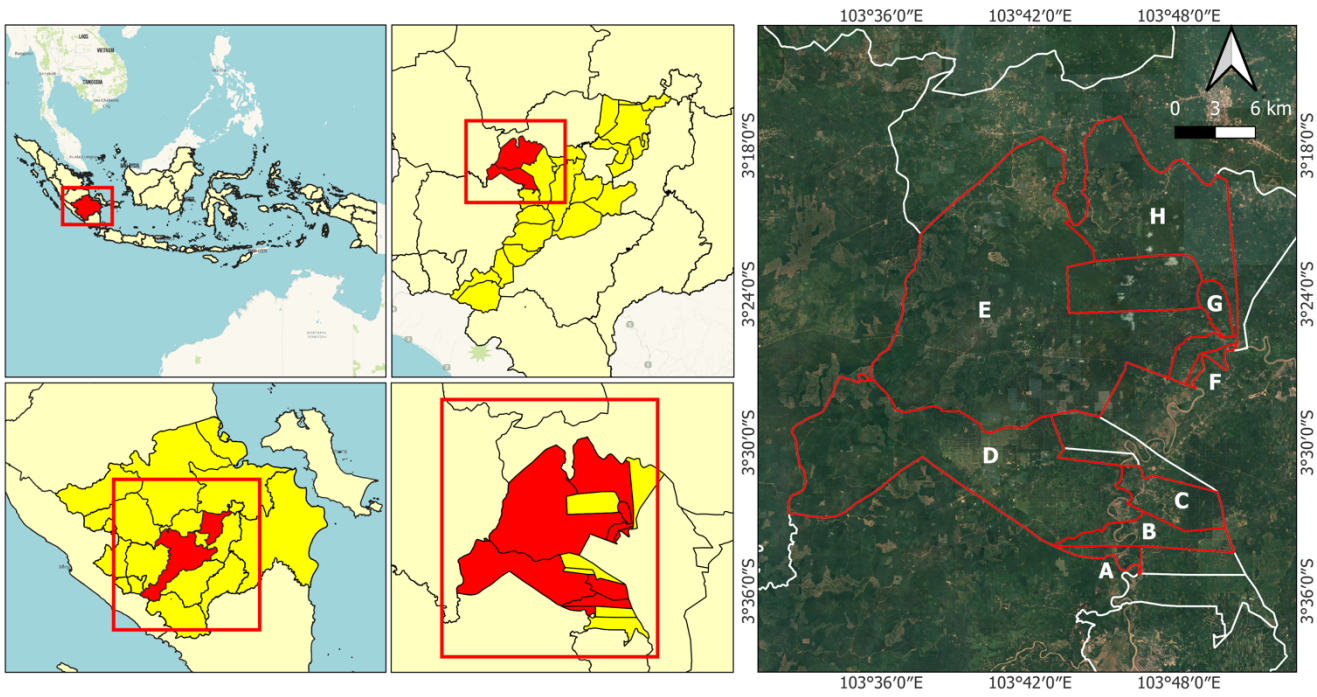

Figure 1. Location study of *Ceratocystis* disease was documented across Muara Enim District, South Sumatra, Indonesia. A. Muara Gula Lama, B. Pinang Belarik, C. Ujan Mas Baru, D. Ujan Mas Lama, E. Padang Bindu, F. Rami Pasai, G. Betung, H. Pagar Dewa

Sample collection

The survey was conducted using a purposive sampling design, focusing on key sub-districts that serve as the primary production centers for *L. domesticum* in Muara Enim. Plots were strategically positioned within these high-incidence zones to ensure sufficient biological material for robust pathogen characterization and to document the epidemic where it is most economically impactful. Since these locations represent the highest density of *duku* orchards in the region, the findings provide a critical reflection of the disease's status in the heart of South Sumatra's *duku* production. While the data in Table 1 specifically characterize these intensive infection zones, they serve as a representative indicator of the lethal wilt impact across the major orchard landscapes (Pratama et al. 2021b, 2025).

The targeted sampling strategy was strategically implemented to maximize the efficiency of isolate collection and to document the pathogen's behavior in the primary *duku* production centers of Muara Enim. By focusing on these high-incidence zones, the study ensures a robust characterization of the epidemic where it is most economically and biologically significant. However, we acknowledge that this purposive placement inherently limits direct statistical comparisons of general orchard epidemiology among villages and constrains the extrapolation of these results to the overall regional prevalence. Instead, the data provide a critical baseline for the disease's maximum impact within the heart of the region's orchard landscapes. A tree was classified as infected if branches or stems exhibited characteristic symptoms, such as bark lesions or wilting. From each affected orchard, five symptomatic *L. domesticum* trees were randomly selected for sapwood tissue collection and subsequent pathogen isolation in the laboratory.

Disease intensity was evaluated using a severity scale from 0 to 4, integrating canopy wilting with the presence of diagnostic stem lesions. To minimize misclassification arising from non-pathogenic factors such as drought or root rot, a tree was only recorded as infected if leaf wilting was accompanied by characteristic *Ceratocystis* symptoms, specifically linear brown-to-black sapwood discolorations or fissured bark. The scoring criteria were defined as follows: Score 0 for healthy trees with no wilted leaves or visible lesions; Score 1 for 1-25% wilted leaves, typically associated with localized lesions on small branches; Score 2 for 25.1-50% wilted leaves with lesions extending toward the main trunk; Score 3 for 50.1-75% wilted leaves, often accompanied by extensive bark cracking and deep sapwood staining throughout the trunk; and Score 4 for 75.1-100% wilted or completely defoliated leaves, indicating systemic colonization of all vascular tissues. By requiring the presence of active stem lesions as a primary diagnostic marker, this assessment ensured that intensity scores accurately reflected the progression of the *Ceratocystis* epidemic rather than non-specific physiological stress. The incidence and intensity of the disease were calculated using the following formula (Chi et al. 2019b; Zhu et al. 2019).

Incidence formula:

$$\text{Disease incidence (DI)} = \frac{\text{number of diseased plants}}{\text{total of trees observed}} \times 100\%$$

Disease intensity formula:

$$\text{Disease severity index (DSI)} = \frac{\Sigma(\text{score} \times \text{number of plants with the score})}{\text{Total number of plants} \times \text{the highest score}} \times 100\%$$

The isolates were collected from fresh *L. domesticum* plants showing symptoms of lesion formation on the sapwood, discoloration of vascular tissues, and partial or total wilting caused by *Ceratocystis.* Sampling was carried out by making incisions in the bark and cutting longitudinal tangential sections (approximately 50 mm) from the newly infected xylem, which appeared dark brown to black. *L. domesticum* trees selected for sampling ranged in age from approximately 20 to 110 years, reflecting the diverse age structure of the heritage orchards in Muara Enim. To ensure a representative collection of the pathogen population, five diseased trees were purposively sampled from each of the 24 orchards (total n = 120), covering the full spectrum of observed disease severity (Scores 1-4) and the recorded age range. Due to the lack of formal plantation records for these ancestral orchards, tree ages were estimated based on farmer interviews. The diseased sapwood samples were immediately wrapped in sterile tissue, placed in labeled plastic bags, and stored in a refrigerator at 4°C before laboratory isolation.

Isolation of *Ceratocystis*

Isolation of *Ceratocystis* was carried out using two complementary methods. The first method involved direct isolation from diseased wood samples cut into 20 × 20 mm segments. These pieces were surface-sterilized by washing in sterile distilled water for 5 minutes, immersing in a streptomycin solution for 5 minutes, followed by 1% sodium hypochlorite (NaClO) for 5 minutes, and a final rinse in sterile distilled water. The sterilized wood pieces were dried in a laminar airflow cabinet and placed on Malt Extract Agar (MEA) at room temperature (25°C) for 7-10 days to induce direct sporulation. The second method utilized the carrot baiting technique (Pratama et al. 2021a, 2021b), where wood samples of the same size were sandwiched between fresh carrot slices and incubated in a moist chamber at room temperature for 6-8 days. A single mass of ascospores developing at the tips of the ascomata on both MEA and carrot slices was transferred onto 2% MEA (20 g/L malt, 20 g/L agar; Biolab, Midrand, South Africa) and incubated for 4-6 days at 25°C.

From a total of 32 isolates collected, eight were selected for detailed analysis, with one representative isolate assigned to each of the eight surveyed locations: C1ME (Ujan Mas Baru), C2ME (Ujan Mas Lama), C3ME (Pinang Belarik), C4ME (Muara Gula Lama), C5ME (Rami Pasai), C6ME (Betung), C7ME (Padang Bindu), and C8ME (Pagar Dewa). To ensure a robust yet unbiased selection, a two-stage screening framework was employed. First, all 32 isolates underwent preliminary morphological and cultural screening, which revealed high uniformity in lesion morphology, radial growth, and sporulation on MEA medium. Statistical validation via One-Way Analysis of Variance (ANOVA)

confirmed no significant differences (P>0.05) in growth rates across the initial pool. Second, from this homogenous pool, one isolate per village was randomly selected using a simple randomization procedure to represent each geographical site. This targeted selection focused on the most robust cultures to ensure reliability in subsequent phylogenetic and pathogenicity testing while maintaining a representative sample size consistent with previous studies on *Ceratocystis* in the region. This sample size was deemed sufficient to test the ITS5 dominance hypothesis, as the observed lack of phenotypic variation strongly suggested a clonal or highly conserved local population (Muslim et al. 2022).

Morphological characterization of *Ceratocystis*

Macroscopic observations were then conducted on these eight isolates to systematically evaluate colony characteristics, pigmentation, and growth rates. Each isolate was replicated four times and incubated at a temperature of 25°C. Subsequently, the colony diameter was measured every 5 days for 20 days, and the average was calculated. Microscopic observations were conducted by examining the morphology of *Ceratocystis* isolates using fungal structures cultured on 2% MEA medium and incubated for 10 days at 25°C. Observations were performed using an Olympus CX33 microscope equipped with an Optilab Advance Plus. To ensure high morphological accuracy and to capture the comprehensive range of structural variability, 100 random observations were recorded for each isolate regarding the length and width of the ascomata (base and neck), ascospores, basiform conidia, barrel-shaped conidia, and chlamydospores. This high-density measurement approach provides a robust descriptive baseline for characterizing the fungal population (Pratama et al. 2021b; Syazwan et al. 2021).

While these 100 observations per structure define the morphological profile within each representative isolate, they were treated as descriptive data to reflect the full phenotypic spectrum of the pathogen in the region. Morphological characters were compared among isolates using One-Way ANOVA for each trait, treating measurements as independent technical replicates, followed by Tukey's Honestly Significant Difference (HSD) test ($\alpha = 0.05$) to detect statistical differences between isolates. While these measurements serve as technical replicates to capture intra-isolate variation, care was taken to sample structures from multiple representative areas of each culture to ensure a robust morphological profile.

Molecular analysis of *Ceratocystis*

Single-spore cultures were prepared from fungal isolates representing each region infected by *Ceratocystis*. The isolates were cultured in Potato Dextrose Broth (PDB) using 250 mL Erlenmeyer flasks at 25°C for 10 days. Mycelia from the PDB cultures were filtered, air-dried, and ground into fine powder using a mortar and pestle. Genomic DNA was extracted using the YeaStar Genomic DNA Kit (Zymo Research Corporation, Irvine, CA, USA). DNA concentration and purity were determined using a NanoDrop ND-1000 spectrophotometer (NanoDrop Technologies, Montchanin, DE, USA).

Polymerase Chain Reaction (PCR) amplification and sequencing were performed for two gene regions: the β-tubulin gene using primers βT1a (`TTC CCC CGT CTC CAC TTC TTC ATG`) and βT1b (`GAC GAG ATC GTT CAT GTT GAA CTC`), and the Internal Transcribed Spacer (ITS) region using primers ITS1 (`TCC GTA GGT GAA CCT GCG G`) and ITS4 (`TCC TCC GCT TAT TGA TAT GC`) (White et al. 1990; Tarigan et al. 2011). PCR reactions (50 µL) consisted of 20 µL Master Mix (Eppendorf, Hamburg, Germany) containing 25 mM $MgCl_2$, 0.06 U/µL Taq DNA polymerase, and 0.2 mM of each dNTP, along with 1 µL of each primer, 1 µL DNA template, and 27 µL sterile water. PCR was performed in a C1000 Touch thermal cycler (Bio-Rad, Hercules, CA, USA) under the following conditions: initial denaturation at 94°C for 3 min; 30 cycles of denaturation at 94°C for 30 s, annealing at 52°C for 30 s, and extension at 72°C for 1 min; followed by a final extension at 72°C for 10 min. Amplified products were stored at 10°C and visualized using a Gel Doc XR+ system (Bio-Rad, Hercules, CA, USA) to verify product size and quality. Verified PCR products were sent to 1st BASE (Selangor, Malaysia) for Sanger sequencing using the same primer sets (Safitri et al. 2025).

Obtained sequences were compared with *Ceratocystis* spp. reference sequences from previous studies and aligned with sequences generated in this study using The Basic Local Alignment Search Tool (BLAST) searches in GenBank (National Center for Biotechnology Information, Bethesda, MD, USA). Sequence alignments were processed in BioEdit v.7.2 (Hall 1999). For phylogenetic metadata, the aligned ITS dataset consisted of approximately 550 bp, while the β-tubulin dataset provided fragments of similar size, with all positions containing gaps and missing data eliminated during analysis. Phylogenetic analyses were conducted using the Maximum Parsimony (MP) method in MEGA v.7 with 1,000 bootstrap replicates. Tree statistics, including tree length, retention index, and consistency index, were calculated to ensure robust branch support (Pratama et al. 2021a, 2021b). *Ceratocystis variospora* was designated as the outgroup, and the ingroup taxa were considered monophyletic.

Koch's postulates and host range test

This study was conducted using eight isolates of *C. fimbriata*. The isolates were selected to represent regions previously affected by *Ceratocystis* disease (Table 1). The inoculation was carried out in two stages. The first inoculation was performed by inoculating the isolates onto *L. domesticum* seedlings to confirm Koch's postulates. Two-year-old *L. domesticum* seedlings were collected from local nurseries in Muara Enim, with stem diameters of 2-3 cm and heights of 50-60 cm. The seedlings were planted in 20 × 20 cm polybags filled with a mixture of soil and manure. All plants were kept in a greenhouse and watered twice daily. The second inoculation test was conducted to determine the host range, using seedlings of plant species that are commonly cultivated or naturally grow around *L. domesticum* orchards, such as *Persea americana*, *Dyera*

costulata, *Archidendron bubalinum*, *Pithecellobium jiringa*, *Eucalyptus* sp., *Durio zibethinus*, *Parkia speciosa*, *Mimusops elengi*, and *Swietenia mahagoni*. The plants used for inoculation were six months old, with stem diameters of 2-3 cm and heights of 40-80 cm. These seedlings were collected from the Forest Plant Nursery Center (BPTH) in South Sumatra, planted in 20 × 20 cm polybags filled with cocopeat, and maintained as described in the first experiment. All experiments were conducted twice to ensure reproducibility, with plants maintained in a greenhouse under a temperature range of 28-32°C and relative humidity of 75-85%.

Inoculation was carried out using isolates grown on 2% MEA medium for 2 weeks. The plant stems were wounded using a sterile cork-borer with a diameter of 4 mm, approximately 10 cm above the soil surface. The inoculation points on the stems were surface-sterilized by wiping with cotton soaked in 75% ethanol. Mycelial plugs of each *Ceratocystis* isolate were taken using a cork borer of the same size (4 mm diameter) and placed into each wound (Pratama et al. 2021a, 2021b). Each isolate was inoculated into 10 seedlings per plant species with the mycelium facing inward, and the same number of plants were used as controls by applying sterile MEA. All inoculated wounds were covered with moistened sterile tissue paper and wrapped with parafilm (Sigma Aldrich, St. Louis, MO, USA) to minimize contamination and drying. The experiments were arranged in a Randomized Complete Block Design (RCBD), with blocks defined by seedling size and greenhouse positioning.

Disease severity and symptoms were observed daily, and the length of internal wood discoloration was measured 60 days post-inoculation (dpi) by peeling the bark at the inoculation point to expose the underlying xylem tissue (Pratama et al. 2025). Pathogenicity levels were categorized into three biologically motivated groups based on a combination of mean lesion lengths and plant mortality rates at 60 dpi. Following the refined methodology of Muslim et al. (2022), isolates were classified as: (i) high pathogenicity (>8.0 cm lesion length and >70% mortality); (ii) moderate pathogenicity (4.0-8.0 cm and 40-60% mortality); and (iii) low pathogenicity (<4.0 cm and <40% mortality). While statistical analyses primarily focused on continuous lesion-length data, this dual-parameter classification was employed to ensure that the categorized pathogenic ability accurately reflects both the aggressive tissue colonization and the ultimate lethal impact of *C. fimbriata* across diverse host species.

Re-isolation from lesion margins was performed using both direct MEA plating and carrot baiting to verify the pathogen's identity via morphological characteristics, thereby fulfilling Koch's postulates. Data for lesion lengths and mortality rates were analyzed using R Studio. Differences among treatments were evaluated using a One-Way Analysis of Variance (ANOVA), followed by Tukey's Honestly Significant Difference (HSD) test ($\alpha = 0.05$) as the consistent post-hoc measure for all pathological parameters.

RESULTS AND DISCUSSION

Field observations and symptom development

A survey across eight major *L. domesticum* production centers revealed that *Ceratocystis* wilt has reached epidemic levels across all studied locations, with both incidence and intensity showing a consistent upward trend between June 2023 and June 2025 (Figure 2, Table 1). At the village level, the rate of progression varied significantly. Ujan Mas Lama experienced the most aggressive spread, transitioning from moderate infection to a maximum incidence and intensity of 100% by the end of the monitoring period. High infection rates were also documented in Pinang Belarik and Ujan Mas Baru, reaching 93.59% and 90.18%, respectively. In contrast, at the plot level, certain sites such as Padang Bindu and Betung maintained notably lower infection rates, concluding the study with incidences below 51%.

The observed variability among orchards indicates that while the pathogen is widespread, the rate of disease progression varies across different sites. A clear correlation emerged between the increase in disease incidence and the escalation of damage severity, particularly during the significant surge observed between July 2024 and June 2025. This trend reflects a rapid epidemic expansion within the surveyed production centers, highlighting the high susceptibility of *L. domesticum* to the *C. fimbriata* ITS5 outbreak in South Sumatra. This progression suggests that once *Ceratocystis* becomes established, it quickly advances to systemic colonization, likely driven by favorable environmental shifts or high vector activity. Specifically, this infection is closely associated with physical injuries to the *duku* trees, such as wounds caused by squirrel feeding and pruning activities during the fruiting season, which create critical entry points that facilitate the rapid spread of the pathogen.

Disease development in the field progressed rapidly, with infected trees typically reaching total mortality within 2-3 months of symptom onset. The infection followed a distinct chronological sequence: initial leaf chlorosis and wilting (Figure 3.A) were followed by total defoliation and canopy death (Figure 3.B). Internal examinations revealed diagnostic bluish-black, scratch-like lesions (Figure 3.C) that extended systemically through the vascular tissues (Figure 3.D). Notably, the disease progression was facilitated by external biotic pressures that created essential entry points for the pathogen. The external surfaces of infected trunks and branches often showed many wounds from squirrel bites (Figures 3.E-3.F) and many small holes were found due to attacks by ambrosia beetles and mango bark beetle (*H. mangiferae*) (Figures 3.G-3.H). These observations, consistent with our previous long-term monitoring (Suwandi et al. 2021; Muslim et al. 2022), confirm that *Ceratocystis* colonization is heavily dependent on such physical injuries and is further accelerated by high vector activity and favorable environmental shifts during the peak infection periods.

Table 1. *Ceratocystis* wilt disease incidence and intensity in *Lansium domesticum* orchard in Muara Enim, South Sumatra, Indonesia

Location (n = Number of plants)	Incidence (%)			Intensity (%)		
	Jun-23	Jul-24	Jun-25	Jun-23	Jul-24	Jun-25
Ujan Mas Baru (n = 112)	49.11	65.18	90.18	47.99	61.61	87.50
Ujan Mas Lama (n = 92)	48.91	67.39	100	44.29	66.85	100
Muara Gula Lama (n = 105)	29.52	51.43	76.19	28.57	50.48	72.38
Pinang Belarik (n = 78)	46.15	67.95	93.59	41.03	64.42	91.67
Rami Pasai (n = 82)	18.29	57.32	75.61	13.72	53.35	72.87
Betung (n = 91)	15.38	30.77	50.55	12.09	27.47	48.08
Padang Bindu (n = 84)	15.48	28.57	48.81	11.90	25.89	47.62
Pagar Dewa (n = 111)	15.32	36.04	54.05	13.74	32.66	52.93

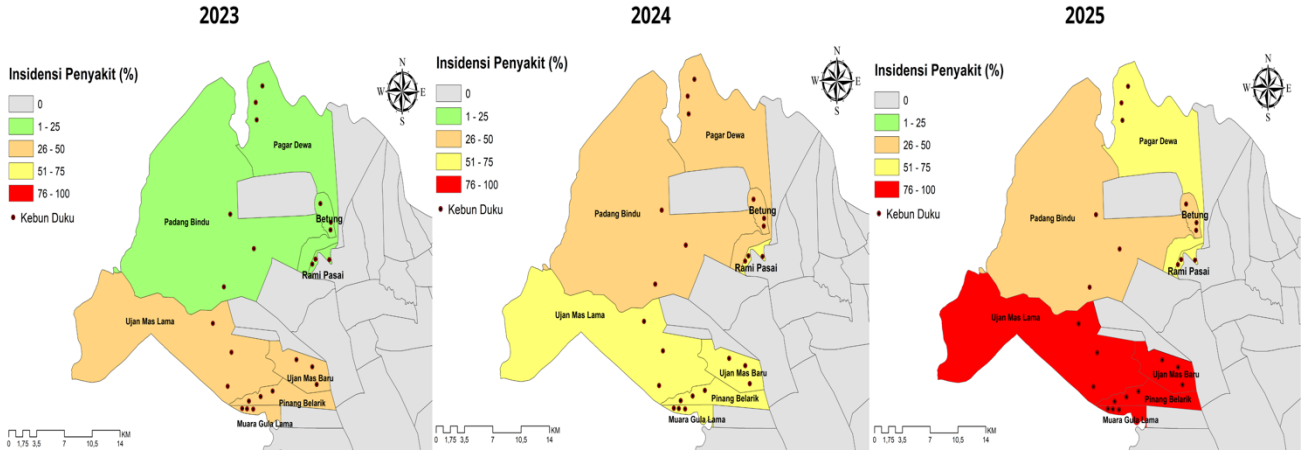

Figure 2. Geographical distribution and temporal progression of *Ceratocystis* wilt in Muara Enim, South Sumatra, Indonesia. Symbols indicate survey point locations, with color gradients representing incidence classes (low to high) based on cumulative data recorded throughout the entire survey period (June 2023, July 2024, and June 2025)

Figure 3. Symptoms of *Ceratocystis* wilt disease on *Lansium domesticum* trees in Muara Enim. A. *Lansium domesticum* trees with wilted and yellowing leaves, B. *Lansium domesticum* leaves that fall off, causing the tree to dry out and die, C-D. Lesions formed on the trunk and branches of infected *Lansium domesticum* trees, E-F. Wounds on the branches and trunk of *Lansium domesticum* trees caused by scratches and bites from squirrels, G. Tunnels produced by *Hypocryphalus mangiferae* on the *Lansium domesticum* tree trunk, H. Adult *Hypocryphalus mangiferae* on the *Lansium domesticum* tree trunk

Culture characteristics and morphology

In this study, carrot baiting proved more efficient, yielding *Ceratocystis*-like colonies from 85% of the samples compared to a 40% success rate for direct MEA plating. Despite the difference in efficiency, all isolates obtained from both methods exhibited identical cultural and morphological characteristics, ensuring the consistency of the pathogen collection for further analysis. A total of 32 isolates were successfully obtained from the eight survey locations. Following comprehensive macroscopic and microscopic observations, eight representative isolates—one from each affected area (C1ME to C8ME)—were selected for further characterization (Figures 4.A-4.H). When grown on MEA, all isolates exhibited morphological features consistent with the genus *Ceratocystis*, including a distinctive banana-like odor and filamentous growth with irregular margins (Table 2). Variations in mycelial color were observed: isolates C1ME, C3ME, C4ME, C5ME, C6ME, and C7ME displayed olive-gray mycelia (Figures 4.A, 4.C-4.G), while C2ME and C8ME showed dark yellowish-brown mycelia (Figures 4.B, 4.H). While these morphological characteristics align with the *C. fimbriata* species complex, they are insufficient to distinguish between specific genotypes or ITS haplotypes. Therefore, molecular sequence analysis was subsequently performed to provide a definitive identification of the ITS5 haplotype and to confirm the genetic identity of the isolates across the surveyed regions.

The radial growth rates of the eight representative *Ceratocystis* isolates (C1ME-C8ME) evaluated and analyzed via one-way ANOVA confirmed that there were no significant differences in colony growth rates among the isolates ($F(7, 24) = 0.72$, $p = 0.66$, $\eta_g^2 = 0.17$) (Figure 5). Macroscopic observations revealed high morphological uniformity among the isolates, with most displaying olive gray colonies (Munsell 5Y 4/2) and a few showing dark yellowish-brown hues (10YR 4/4) (Table 2). All isolates exhibited moderate growth with filamentous forms and irregular margins. This phenotypic consistency across different geographical origins in Muara Enim suggests a relatively homogenous population within the surveyed regions. Such morphological stability is a common characteristic of *C. fimbriata* isolates associated with localized outbreaks, providing a baseline for the subsequent molecular identification and haplotype analysis.

Table 2. Characteristics of *Ceratocystis* colonies from *Lansium domesticum* plants in Muara Enim

Origin (isolate code)	Colony color	Munsell code	Growth pattern	Form	Margin
Ujan Mas Baru (C1ME)	Olive gray	5Y;4/2	Moderate	Filamentous	Irregular
Ujan Mas Lama (C2ME)	Dark yellowish brown	10YR;4/4	Moderate	Filamentous	Irregular
Pinang Belarik (C3ME)	Olive gray	5Y;4/2	Moderate	Filamentous	Irregular
Muara Gula Lama (C4ME)	Olive gray	5Y;4/2	Moderate	Filamentous	Irregular
Rami Pasai (C5ME)	Olive gray	5Y;4/2	Moderate	Filamentous	Irregular
Betung (C6ME)	Olive gray	5Y;4/2	Moderate	Filamentous	Irregular
Padang Bindu (C7ME)	Olive gray	5Y;4/2	Moderate	Filamentous	Irregular
Pagar Dewa (C8ME)	Dark yellowish brown	10YR;4/4	Moderate	Filamentous	Irregular

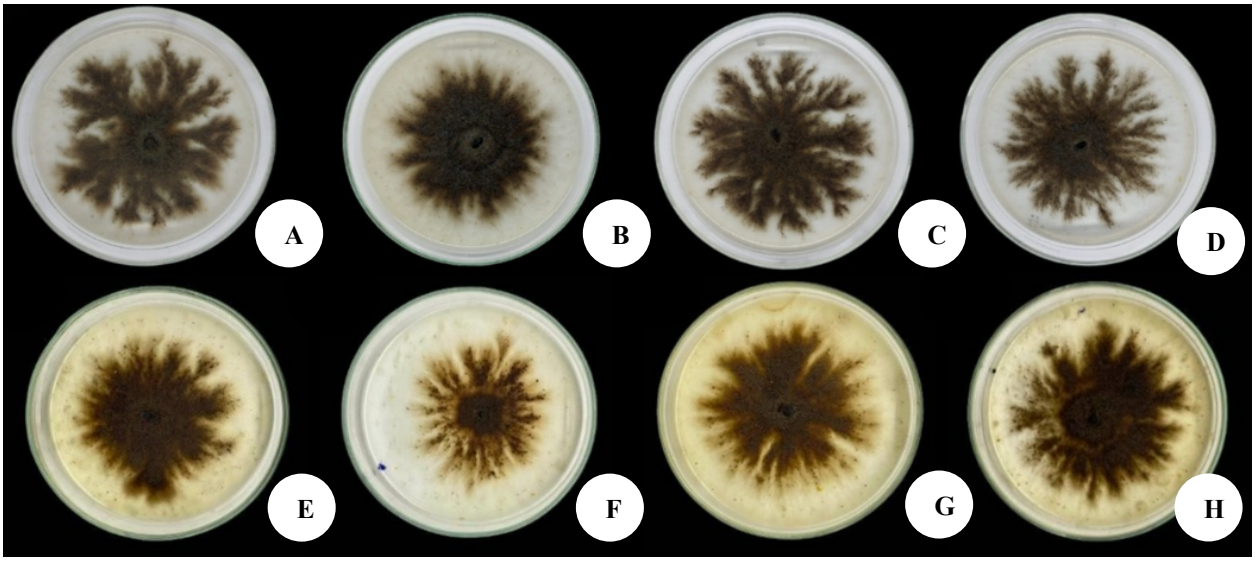

Figure 4. Morphological characteristics of *Ceratocystis fimbriata* isolates from Muara Enim, South Sumatra. A-H. Macroscopic colony morphology of isolates C1ME to C8ME (C: *Ceratocystis*, ME: Muara Enim) after 7-10 days of incubation on 2% Malt Extract Agar (MEA) medium at room temperature (25±2°C). Colonies exhibit typical olive-gray to dark yellowish-brown coloration with filamentous growth and irregular margins

All isolates have globose to sub-globose ascomata (Figures 6.1.A-6.1.H) with long necks and characteristic divergent ostiolar hyphae at the tip (Figures 6.2.A-6.2.H). The teleomorph and anamorph structures were produced within 2 weeks on MEA culture. All isolates have ascomatal bases that are dark brown to black, with subglobose to globose shapes and measuring 170.83±22.83-212.36±41.26 × 164.90±57.7-246.16±65.90 µm. Ascomatal necks are erect, occasionally curved, black at the base and becoming subhyaline toward the apex, smooth to crenulate, 359.54±93.1-489.89±98.11 µm long including ostiolar hyphae. Phialides are pale brown to hyaline (Figures 6.3.A-6.3.H). All isolates possess two distinct types of hyaline conidia: cylindrical, measuring 26.04±3.25-33.06±10.61 × 4.35±0.68-6.54±1.79 µm (Figures 6.4.A-6.4.H), and barrel-shaped, measuring 8.38±2.34-10.28±5.94 × 5.12±0.51-6.48±1.66 µm. All isolates have hyaline ascospores measuring 6.21±0.69-9.77±1.63 × 3.73±0.98-5.80±1.05 µm (Figures 6.5.A-6.5.H), and aleuroconidia or chlamydospores with thick walls, oval shape, and smooth surfaces, occurring singly or in basipetal chains, measuring 12.01±7.48-13.98±1.41 × 9.19±3.03-11.53±6.55 µm (Figures 6.6.A-6.6.H). Based on the analysis of morphological measurements (Table 3), all isolates are typical of *Ceratocystis* spp. within the *C. fimbriata* sensu lato species complex.

Sequence analyses

The resulting sequences (C1ME-C8ME) were submitted to GenBank and assigned Accession Nos. PX854836-PX854843 for the ITS region and PX883859-PX883866 for β-tubulin. While the ITS sequences among the eight isolates differed by two bases (99.6% similarity), manual alignment with previously characterized genotypes confirmed that all isolates consistently match the ITS5 haplotype. In contrast, the β-tubulin sequences were completely identical (100% similarity) across all isolates. This lack of variation in the more conserved β-tubulin gene, combined with the shared ITS5 haplotype, is suggestive of low detected genetic variation under the current molecular markers. While these results align with the patterns typically observed during rapid outbreaks, the uniformity across the ITS and β-tubulin loci indicates a highly conserved population in the region, rather than a definitively confirmed clonal expansion.

BLAST searches for both the ITS and β-tubulin regions confirmed their identity as *C. fimbriata* with 100% similarity and query coverage against GenBank entries. Maximum Parsimony (MP) analysis of the β-tubulin sequences yielded a single most parsimonious tree (76 steps, CI = 0.9375, RI = 0.9784, Figure 7), while the ITS analysis resulted in a tree of 62 steps (CI = 0.5937, RI = 0.8737, Figure 8). *Ceratocystis* isolates from *Lansium* in Indonesia were placed within the Latin American Clade (LAC) of *C. fimbriata sensu lato*, clustering closely with the ex-type and ex-paratype isolates of *C. manginecans*—a taxon currently regarded as conspecific with *C. fimbriata sensu stricto* (Harrington et al. 2014; Oliveira et al. 2015).

The high bootstrap support values (e.g., >90%) for the clade containing our isolates and the ITS5 references indicate a robust phylogenetic placement, confirming that the *Lansium* epidemic is driven by this globally dominant genotype. This is consistent with the known behavior of the ITS5 haplotype, which has been reported on diverse hosts such as *Eucalyptus*, *Acacia*, and *Punica* worldwide. Our findings reinforce the role of the ITS5 haplotype as a major driver of *Ceratocystis* epidemics across various commodities, characterized here by a clear clonal lineage.

Koch's postulate and host range test

Lansium domesticum seedlings inoculated only with blank MEA showed no symptoms of disease; their leaves did not wilt and remained green, and no lesion spots were found in the sapwood or vascular tissues (Figures 9.A, 9.C, 9.D). In contrast, *L. domesticum* plants inoculated with *Ceratocystis* isolates exhibited typical symptoms of *Ceratocystis* infection, characterized by wilting, yellowing and drying of the leaves, eventually leading to plant death, along with the formation of dark brown to blackish lesions in the sapwood and vascular tissues (Figures 9.B, 9.E, 9.F).

The leaves of *L. domesticum* plants inoculated with *Ceratocystis* began to show wilting symptoms at 45 Days After Inoculation (DAI), initially characterized by yellowing, which progressed to browning and eventual desiccation. In contrast, control plants remained asymptomatic with healthy green foliage throughout the observation period. By 60 DAI, the infection rate reached 100%, as evidenced by the successful colonization and development of necrotic lesions in all inoculated seedlings, with lesion lengths ranging from 3.97 to 12.31 cm (Table 4). Statistical analysis confirmed that these lesion lengths were significantly different ($P<0.05$) from the control seedlings treated with sterile MEA, which showed no wood discoloration. While infection was universal across all inoculated plants, plant mortality varied among isolates, with death rates ranging from 30% to 90%. To fulfill Koch's Postulates, *Ceratocystis* was successfully re-isolated from the symptomatic tissues of all inoculated plants, whereas no fungal pathogens were recovered from the controls.

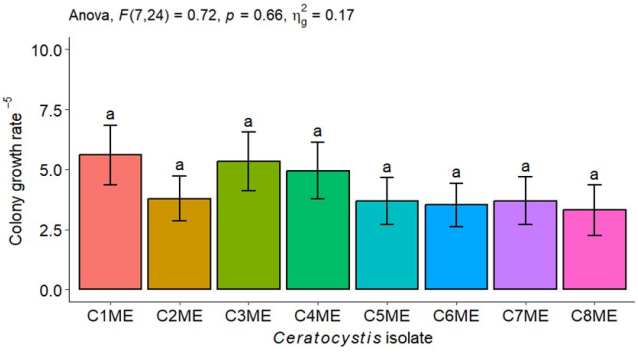

Figure 5. Mean colony growth rates of eight *Ceratocystis fimbriata* isolates (C1ME-C8ME) cultured on 2% Malt Extract Agar (MEA). The vertical axis represents the growth rate (mm/day), while error bars indicate the Standard Deviation (SD) of the mean. Letters above the bars indicate statistical groupings based on Tukey's HSD test ($\alpha = 0.05$). One-way ANOVA showed no significant differences in growth rates among all isolates ($p = 0.66$)

Table 3. Morphology of selected *Ceratocystis fimbriata* isolates from Muara Enim District

Morphology[a]	C1ME	C2ME	C3ME	C4ME	C5ME	C6ME	C7ME	C8ME
Perithecial base width	206.52±45.95b	173.59±27.01a	246.16±65.90c	173.66±41.68a	165.58±34.16 a	200.60±41.8 b	177.97±31.37a	164.90±57.7 a
Perithecial base length	207.50±45.50b	170.83±22.83a	230.47±60.41b	175.55±43.27a	183.01±40.8 a	212.36±41.26b	187.50±30.6 a	173.38±58.11b
Neck length	489.89±98.11a	449.37±71.03a	474.96±76.55a	460.04±96.68a	360.57±105.4 a	399.37±91.06a	361.19±88.3 a	359.54±93.1 a
Neck width base	30.95±4.89ab	31.01±6.99ab	32.16±7.27b	28.32±5.29a	28.34±5.55 a	31.78±6.31 ab	31.73±4.7 ab	33.62±10.5 b
Neck width tip	17.34±3.50a	18.20±4.33ab	19.67±3.75b	17.22±3.06a	17.32±3.71 a	17.26±3.19 a	17.17±3.67 a	17.24±8.54 a
Ascospore length	6.23±0.56a	6.30±0.78a	6.27±0.56a	6.21±0.69a	8.52±1.45 b	8.99±1.37 b	9.77±1.63 c	8.77±1.51 b
Ascospore width	5.80±1.05c	5.22±1.18bc	5.41±1.10bc	5.41±0.94bc	4.61±1.00 b	4.31±0.81 b	3.73±0.98 a	3.77±1.11 a
Cylindrical conidia. length	26.52±3.28a	28.91±5.03b	26.04±3.25a	27.28±2.06ab	26.95±10.13 a	31.94±10.70 bc	33.06±10.61 c	27.65±7.14 ab
Cylindrical conidia. width	4.93±0.75ab	4.62±0.53ab	5.08±1.18b	4.35±0.68a	4.42±1.68 a	4.66±1.83 ab	6.54±1.79 c	6.05±2.02 c
Barrel conidia. length	9.50±2.59b	8.75±2.35a	8.87±2.24a	8.38±2.34a	8.64±4.77 a	10.28±5.94 b	9.16±5.01 ab	8.42±4.20 a
Barrel conidia. width	5.14±0.51a	6.07±0.69ab	6.48±1.66b	5.12±0.51a	6.31±1.67 b	5.31±1.70 a	6.16±1.55 ab	5.97±1.54 ab
Chlamydospore. length	12.07±1.18a	13.13±1.25b	13.33±1.38b	13.98±1.41b	12.15±10.91 a	13.52±23.06 b	12.8±7.53 a	12.01±7.48 a
Chlamydospore. width	9.70±1.01a	10.95±1.31b	10.21±1.12a	10.89±1.17b	11.53±6.55 c	9.19±3.03 a	10.47±6.35 b	10.02±3.27 ab
Hyphal. length	60.23±19.63a	58.75±13.23a	61.70±11.54a	65.59±15.81a	20.08±3.41 ab	21.27±3.02 bc	18.04±4.07 a	22.32±6.06 c
Hyphal. width	15.09±3.54a	17.59±2.73b	19.13±5.13b	14.84±3.14a	10.91±2.82 a	11.75±3.00 a	10.62±2.83 a	14.32±4.94 b

Note: [a]All morphological measurements are presented as the mean±Standard Deviation (SD) based on 100 observations per structure for each isolate. In the table, values followed by different lowercase letters within a row indicate significant differences between isolates according to Tukey's Honestly Significant Difference (HSD) test at $\alpha = 0.05$. All structural dimensions, including the length and width of the ascomata, ascospores, conidia, and chlamydospores, are expressed in micrometers (μm)

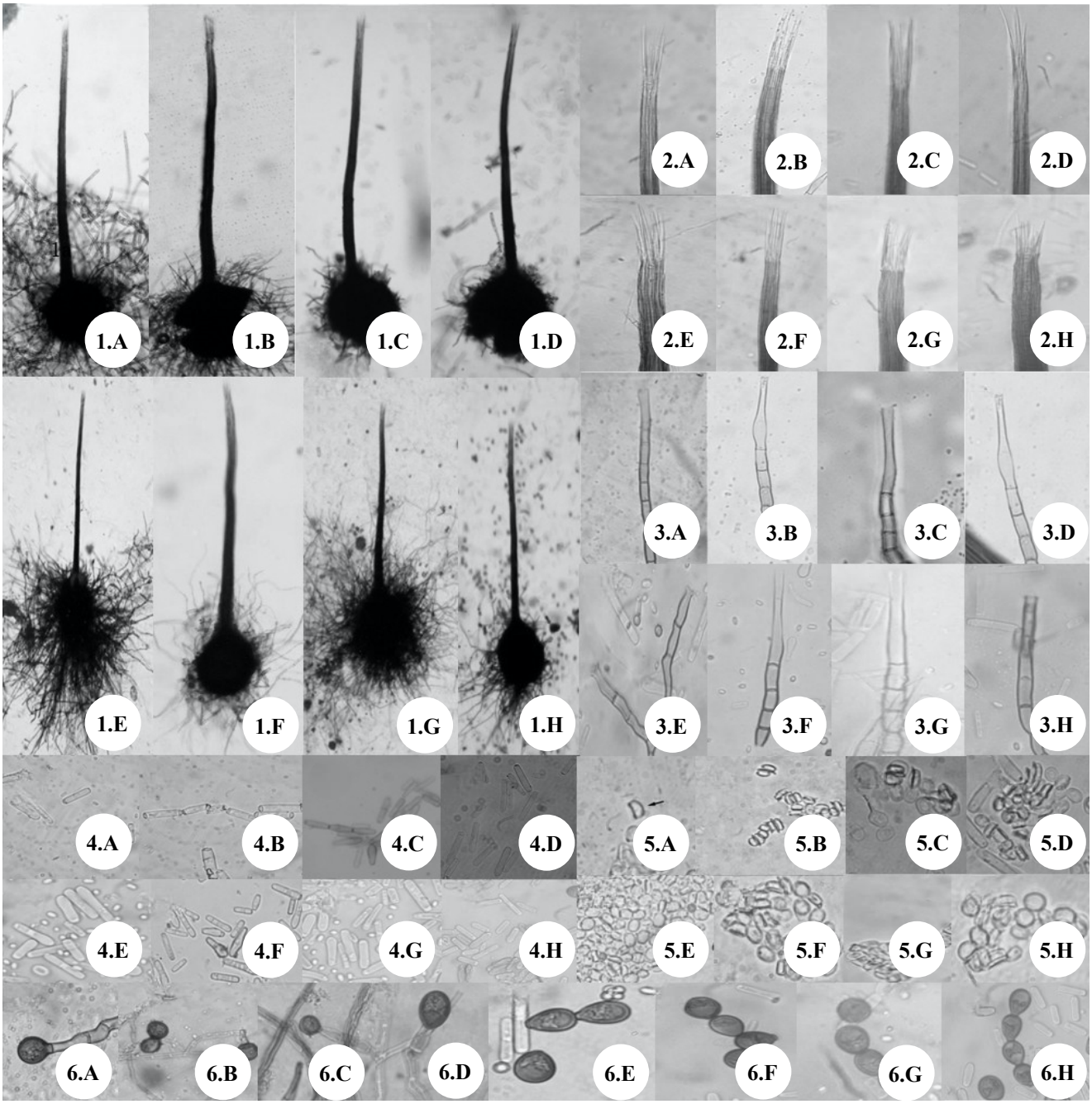

Figure 6. Morphology of *Ceratocystis fimbriata*. 1.A-1.H. Perithecial-shaped ascomata, 2.A-2.H. Divergent ostiolar hyphae, 3.A-3.H. Conidiophore/phialide, 4.A-4.H. Cylindrical conidia, 5.A-5.H. Hat-shaped ascospores, 6.A-6.H. Chlamydospores. A-H. C1ME-C8ME. Scale bars: a: 100 µm, b, c, e, f: 5 µm, d: 5 µm

The host range assay demonstrated that all *C. fimbriata* isolates were capable of infecting a wide variety of plant species, producing necrotic lesions comparable to those observed in the primary host, *L. domesticum* (Figure 10). Pathogenicity levels were categorized based on mean lesion lengths 60 days post-inoculation: high pathogenicity (>8.0 cm and percentage of mortality >70%), moderate pathogenicity (4.0-8.0 cm and percentage of mortality 40-60%), and low pathogenicity (<4.0 cm and percentage of mortality <40%). Based on these criteria, the isolates exhibited high pathogenicity on *P. speciosa* (4.67±2.12c to 11.08±3.08 cm and mortality percentage is 60-70%) and *P. americana* (4.80±0.65 to 9.06±1.13 cm and mortality percentage is 60-90%). Moderate pathogenicity on *Durio* sp. (2.63±0.51 to 7.89±1.25 cm and mortality percentage is 30-50%), *A. bubalinum* (3.67±1.95 to 5.19±0.64 and mortality percentage is 30-60%), *P. jiringa* (3.56±0.80 to 8.89±1.24 and mortality percentage is 40-60%), *M. elengi* (4.65±1.49 to 7.52±1.02 and mortality percentage is 30-60%), and *S. mahagoni* (2.33±1.25 to 6.01±0.67 and

mortality percentage is 40-50%). Low pathogenicity was observed on *D. costulata* (3.65±0.94c to 6.34±1.22 and mortality percentage is 20-30%), where lesions and mortality percentage remained localized (Tables 5 and 6). Analysis of Variance (ANOVA) indicated that lesion lengths across all inoculated hosts were significantly different from the control plants, which remained symptomless. Further analysis using Tukey's HSD test (α= 0.05) revealed that while lesion lengths varied significantly among most treatments, no significant differences in susceptibility were detected among isolates when inoculated onto *A. bubalinum*.

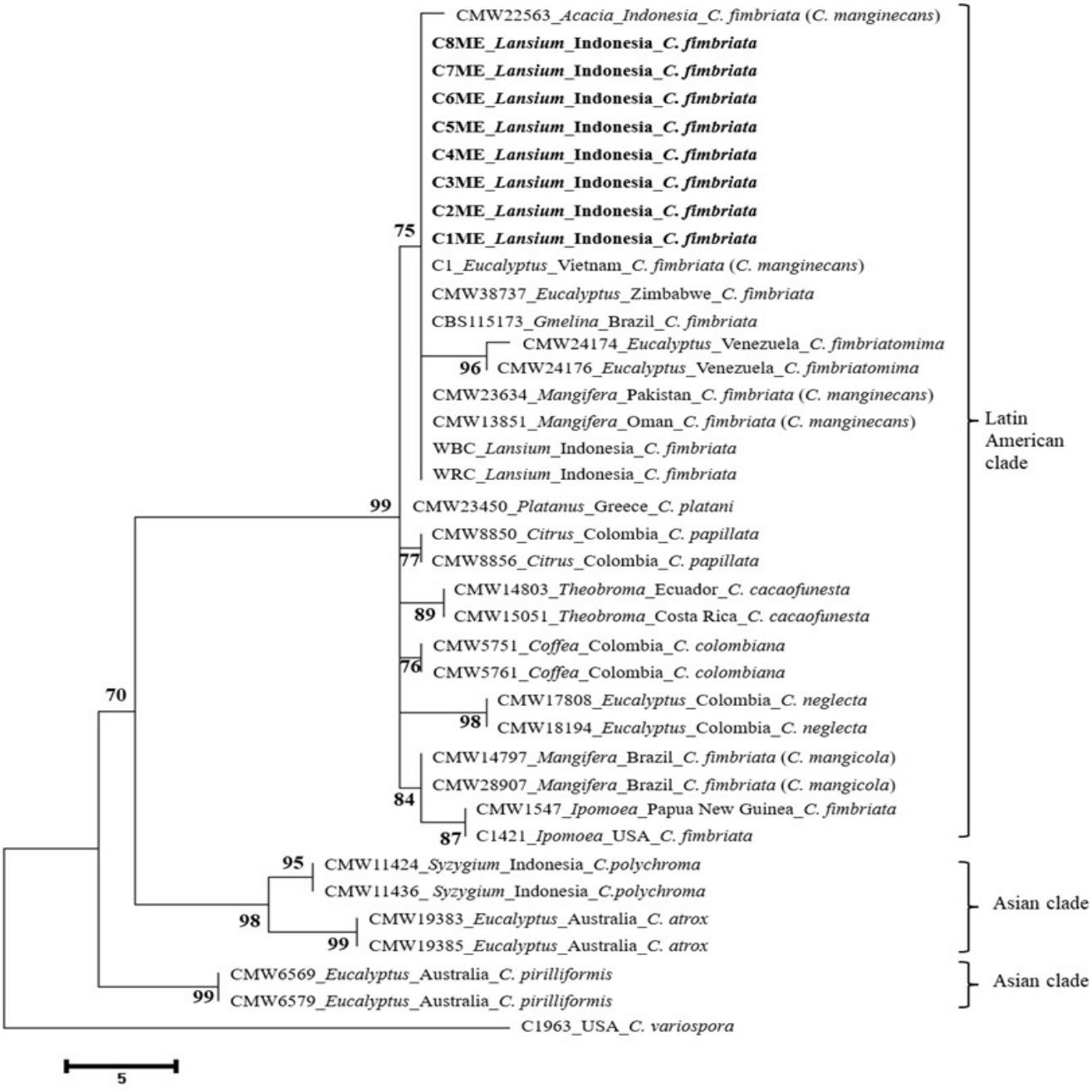

Figure 7. Phylogenetic tree inferred from maximum parsimony analysis of β-tubulin gene sequences, illustrating the phylogenetic relationship between *Ceratocystis fimbriata* isolated from *Lansium* trees in Indonesia (indicated in bold) and other taxa within the Latin American and Asian clade of the *Ceratocystis fimbriata* species complex. Strain identifiers, host genera, countries of origin, and corresponding species names are provided for each representative isolate. Species regarded as synonyms of *Ceratocystis fimbriata* sensu stricto are shown in parentheses (Harrington et al. 2014; Oliveira et al. 2015). *Ceratocystis variospora* was designated as the outgroup taxon. Bootstrap support values exceeding 50%, based on 1,000 replicates, are displayed at the corresponding nodes

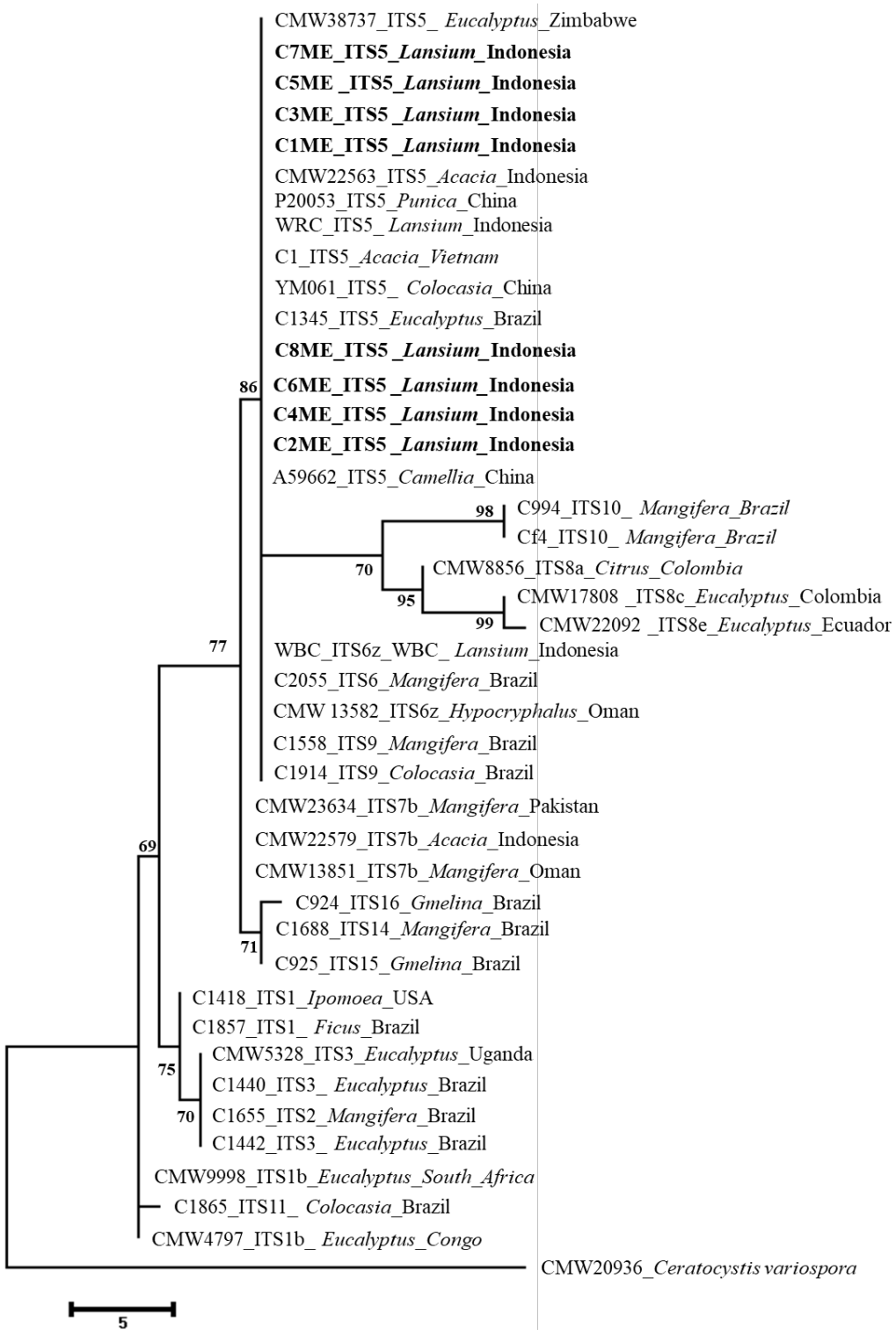

Figure 8. Dendrogram generated by maximum parsimony analysis showing the genetic relatedness of representative internal transcribed spacer (ITS) rDNA genotypes (sequences) of *Ceratocystis fimbriata* sensu stricto. The strain numbers, ITS haplotypes, host genera, and countries of origin are provided for representatives of each haplotype. Isolates from *Lansium domesticum* in Indonesia are indicated in bold. The ITS haplotypes of *Ceratocystis fimbriata* are numbered according to the numerical designations of Harrington et al. (2014). *Ceratocystis variospora* was used as the outgroup taxon. Bootstrap values greater than 50%, obtained from a bootstrap test with 1,000 replications, are indicated on the corresponding nodes. The scale bar represents genetic distance

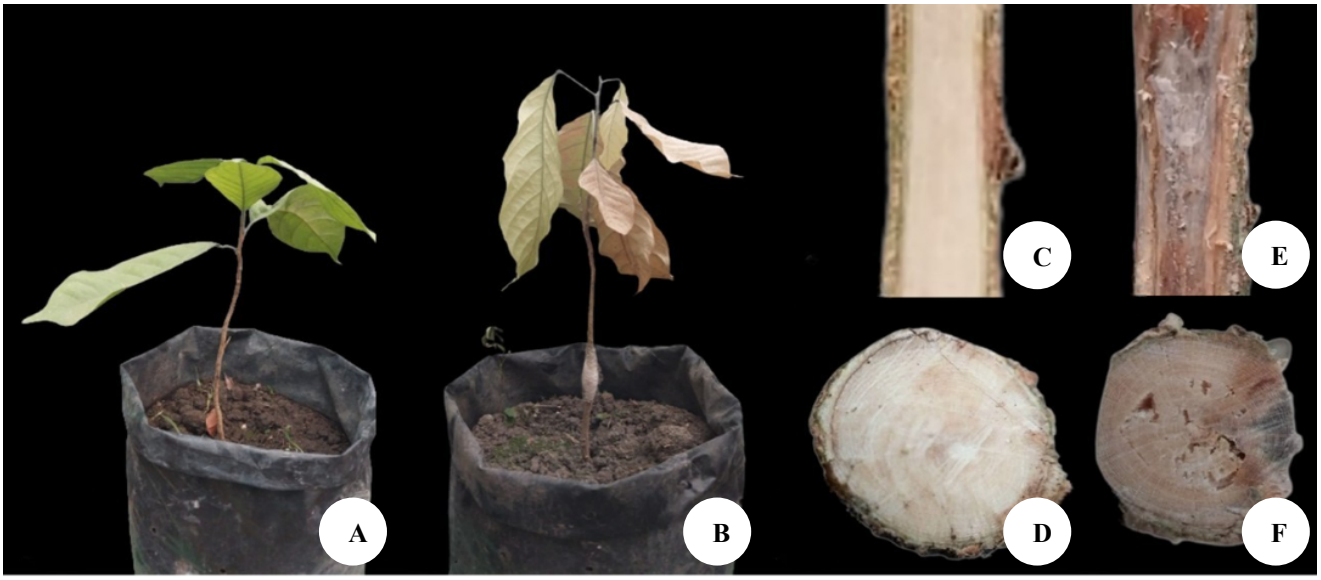

Figure 9. Koch's postulate test on two-year-old *Lansium domesticum* seedlings. A. Healthy *Lansium domesticum* seedlings as control inoculated only with MEA, B. Leaves showing wilting and drying symptoms on *Lansium domesticum* seedlings inoculated with *Ceratocystis*, C-D. No lesions formed on the sapwood and heartwood of control *Lansium domesticum* seedlings, E-F. Lesions found on the sapwood and heartwood of *Lansium domesticum* seedlings inoculated with *Ceratocystis* isolates

Table 4. Koch's postulate test and the pathogenicity of *Ceratocystis fimbriata* on *Lansium domesticum*

Treatments	Number of test plants	*Lansium domesticum*	
		Length of lesion (cm)	Dead plants
C1ME	10	4.42±1.70b	5/10
C2ME	10	3.97±1.17b	4/10
C3ME	10	4.22±1.18b	5/10
C4ME	10	7.28±2.19bc	3/10
C5ME	10	8.63±1.87bc	4/10
C6ME	10	12.31±1.46c	9/10
C7ME	10	8.90±2.00bc	6/10
C8ME	10	9.02±1.67bc	7/10
Control	10	0a	0/10
p-value		0.012	

[a]Values followed by the same letter in the same column are not significantly different among isolates at P = 0.05 according to Tukey's Honest Significant Difference (HSD) multiple range test

Discussion

Monitoring data from 2023 to 2025 reveals a significant intensification in the *Ceratocystis* epidemic within Muara Enim, transitioning from the localized riparian mortality reported in 2014 to extensive tree loss in several surveyed orchards. With incidence reaching 100% in hubs such as Ujan Mas Lama, this surge—from less than 12% in 2021 to near-complete destruction in certain sites by 2025—indicates a substantial escalation of the disease. Molecular evidence from the representative isolates identifies the ITS5 haplotype of *C. fimbriata* as the primary genotype associated with this escalation, further supporting previous links between this genotype and mass *L. domesticum* mortality across South Sumatra (Suwandi et al. 2021; Muslim et al. 2022). While ITS5 is globally recognized as a virulent lineage across diverse crops, the Muara Enim outbreak is distinguished by the rapid systemic collapse of trees within six months, representing a severe regional manifestation of a global threat. The rapid escalation of the disease in Muara Enim is driven by a synergistic mechanism involving biotic vectors, environmental conduits, and poor phytosanitary practices. The role of *H. mangiferae* and other ambrosia beetles (e.g., *Xyleborus* spp.) is pivotal; their boring activity, attracted by fungus-induced "banana-like" volatiles, facilitates the rapid movement of propagules from diseased to healthy tissues (Roy et al. 2020; Syazwan et al. 2021; Lynn et al. 2025). This is exacerbated by the presence of squirrels whose gnawing creates infection entry points (Muslim et al. 2022). Furthermore, the farmers' practice of leaving infected dead trees unremoved creates massive inoculum reservoirs. These standing "inoculum factories" produce aleurioconidia dispersed via wind-borne sawdust (Roy et al. 2018) or contaminated pruning tools (Chi et al. 2019a), while river systems act as secondary conduits for waterborne spores, explaining the heightened severity in orchards near water bodies. In alignment with the study's primary objectives, our results experimentally confirm the high virulence of *L. domesticum*-derived ITS5 isolates and their significant host-infecting plasticity. We demonstrated that the pathogen successfully infects distantly related but economically vital species, such as *P. speciosa* and *P. americana*, causing substantial vascular lesions. This broad pathogenicity confirms that the Muara Enim epidemic is not restricted to a single host but poses a systemic risk to the biodiversity and economic stability of polyculture systems in South Sumatra. These findings underscore the urgent need for biosecurity measures that extend beyond *duku* monocultures to protect the region's broader agroforestry landscape from this aggressive clonal lineage.

The isolates obtained from Muara Enim District exhibited morphological characteristics identical to those previously reported from other *L. domesticum* production centers. Colonies appeared olive gray to dark yellowish brown with filamentous growth and a distinctive banana-like aroma, producing ascomata (perithecia), conidiophores, chlamydospores, and hat-shaped ascospores (Muslim et al. 2025; Pratama et al. 2026). Molecular characterization based on ITS and β-tubulin confirmed a 99% similarity to *C. fimbriata*. While previous studies identified sequence variations and multiple haplotypes such as ITS6z (Suwandi et al. 2021) and ITS7b (Muslim et al. 2022) across South Sumatra, our analysis of eight isolates from Muara Enim showed that all isolates examined so far belong to haplotype ITS5. Although this suggests ITS5 is the dominant driver of the current epidemic, wider sampling across diverse micro-environments remains necessary to definitively exclude the presence of additional haplotypes.

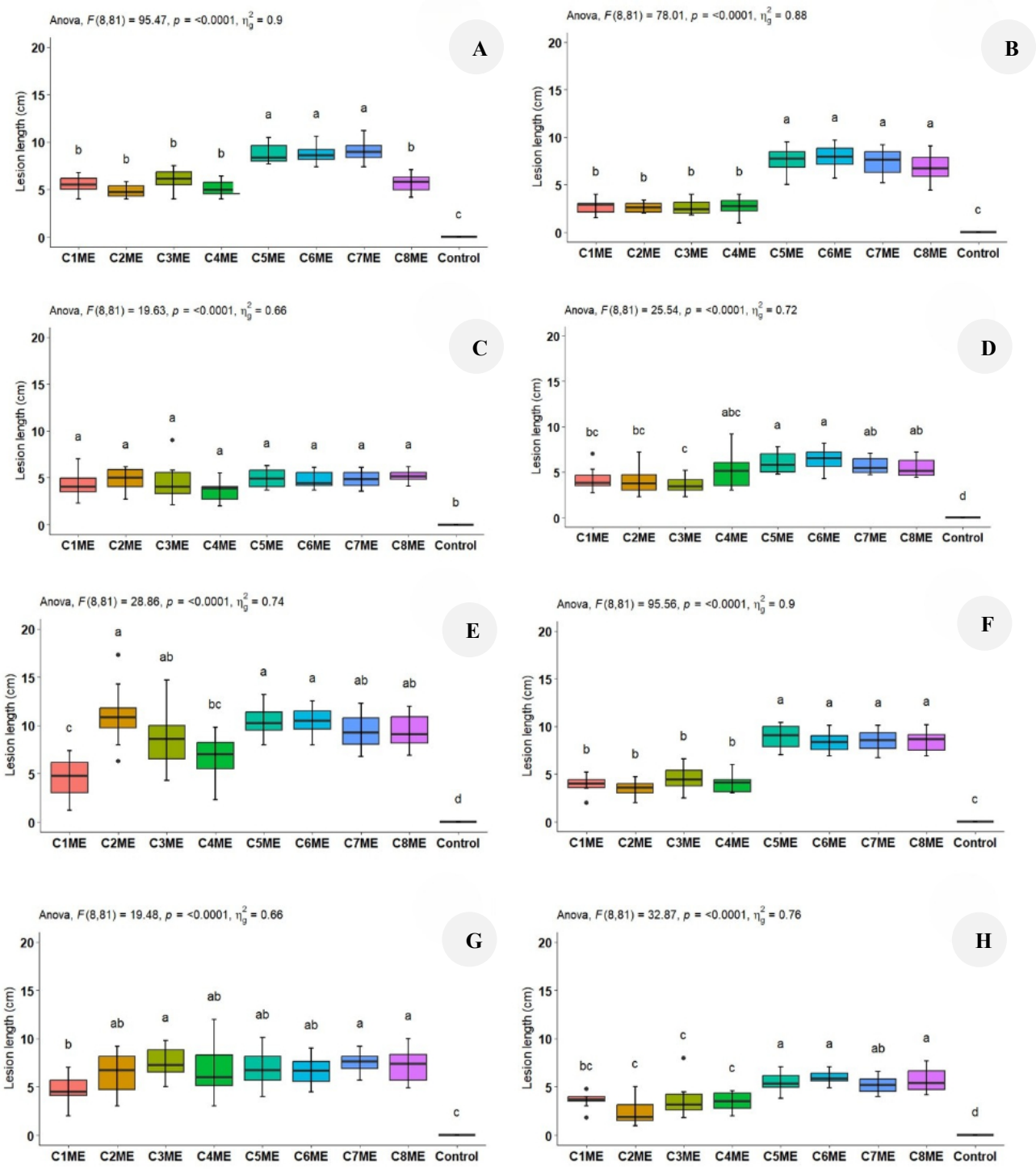

Figure 10. Boxplots of lesion length on host range test plants. A. *Persea americana*, B. *Durio* sp., C. *Archidendron bubalinum*, D. *Dyera costulata*, E. *Pithecellobium jiringa*, F. *Parkia speciosa*, G. *Mimusops elengi*, H. *Swietenia mahagoni*

Table 5. Lesion length on host-range test plants at 60 days post-inoculation (dpi)

Treatments	Number of test plants	Length of lesion (cm)							
		Persea americana	***Durio* sp.**	***Archidendron bubalinum***	***Dyera costulata***	***Pithecellobium jiringa***	***Parkia speciosa***	***Mimusops elengi***	***Swietenia mahagoni***
C1ME	10	5.53±0.95b	2.72±0.76b	4.32±1.51a	4.17±1.25bc	3.95±0.90b	4.67±2.12c	4.65±1.49b	3.68±0.86bc
C2ME	10	4.80±0.65b	2.63±0.51b	4.87±1.20a	4.01±1.45bc	3.56±0.80b	11.08±3.08a	6.45±2.23ab	2.33±1.25c
C3ME	10	6.05±1.03b	2.66±0.83b	4.56±1.95a	3.65±0.94c	4.51±1.12b	8.64±3.07ab	7.45±1.57a	3.64±1.78c
C4ME	10	5.11±0.84b	2.72±0.87b	3.67±1.95a	5.14±1.98abc	4.05±0.97b	6.61±2.29bc	6.76±2.56ab	3.49±0.96c
C5ME	10	8.79±1.03a	7.54±1.37a	4.94±0.99a	6.04±0.36a	8.89±1.24a	10.42±1.66a	6.92±2.00ab	5.54±0.97a
C6ME	10	8.78±0.99a	7.89±1.25a	4.81±0.91a	6.34±1.22a	8.34±0.99a	10.50±1.43a	6.66±1.42ab	6.01±0.67a
C7ME	10	9.06±1.13a	7.37±1.37a	4.85±0.87a	5.69±0.88ab	8.50±1.08a	9.44±1.87ab	7.52±1.02a	5.18±0.87ab
C8ME	10	5.65±0.99b	6.81±1.44a	5.19±0.64a	5.53±1.03ab	8.49±1.11a	9.44±1.74ab	7.24±1.76a	5.76±1.30a
Control	10	0.00c	0.00c	0.00b	0.00d	0.00c	0.00d	0.00c	0.00d
p-value		<0.0001	<0.0001	<0.0001	<0.0001	<0.0001	<0.0001	<0.0001	<0.0001

Table 6. Mortality on host-range test plants at 60 days post-inoculation (dpi)

Treatments	Number of test plants	Dead plants							
		Persea americana	***Durio* sp.**	***Archidendron bubalinum***	***Dyera costulata***	***Pithecellobium jiringa***	***Parkia speciosa***	***Mimusops elengi***	***Swietenia mahagoni***
C1ME	10	7/10	4/10	5/10	2/10	4/10	7/10	5/10	4/10
C2ME	10	7/10	5/10	6/10	2/10	5/10	7/10	6/10	5/10
C3ME	10	6/10	3/10	6/10	3/10	5/10	6/10	4/10	4/10
C4ME	10	9/10	5/10	5/10	3/10	4/10	7/10	6/10	3/10
C5ME	10	9/10	5/10	3/10	2/10	5/10	6/10	3/10	2/10
C6ME	10	7/10	3/10	3/10	2/10	4/10	8/10	5/10	3/10
C7ME	10	7/10	5/10	4/10	2/10	5/10	7/10	3/10	2/10
C8ME	10	6/10	4/10	5/10	2/10	6/10	6/10	4/10	4/10
Control	10	0/10	0/10	0/10	0/10	0/10	0/10	0/10	0/10
p-value		<0.0001	<0.0001	<0.0001	<0.0001	<0.0001	<0.0001	<0.0001	<0.0001

Globally, ITS5 is recognized as the most prevalent haplotype of *C. fimbriata* sensu stricto, affecting various hosts including *Eucalyptus* spp. and *M. indica* in Southeast Asia (Tarigan et al. 2011; Trang et al. 2018), Brazil (Harrington et al. 2014), and Zimbabwe (Jimu et al. 2015). The uniformity of this haplotype in our study leads us to hypothesize a rapid clonal expansion at the regional scale, where a highly aggressive lineage has successfully established itself within Muara Enim. This is consistent with the observation of complete mortality within the severely affected orchards surveyed during the 2023-2025 period. These findings align with Harrington et al. (2014), who described ITS5 as a phylogenetically cohesive and aggressive group with high dissemination potential. Similar patterns in China—where ITS5 drives outbreaks in crops like pomegranate (*Punica granatum*) and tea plant (*Camellia sinensis*) (Li et al. 2016; Xu et al. 2019)—further suggest that while this genotype represents a stable and invasive lineage of global significance, its current dominance in South Sumatra likely reflects a specialized, highly virulent clonal sweep.

Koch's postulate and pathogenicity assays demonstrated that *C. fimbriata* isolates obtained from *L. domesticum* exhibited high virulence, with an infection rate of 100%, resulting in progressive wilting and eventual plant death. Highly pathogenic isolates, namely C6ME and C8ME, were capable of inducing extensive stem lesions and caused complete mortality of all inoculated plants within 90 days post-inoculation. The symptomatology observed in the inoculated plants was consistent with field observations, thereby reinforcing the role of *C. fimbriata* as the primary causal agent of mortality in *duku*. Artificial inoculation conducted at a distance of 10 cm from the stem base led to the death of the entire plant, with the pathogen capable of vertical movement exceeding 9 cm both upward and downward from the inoculation site. This pattern is characteristic of vascular wilt diseases, in which pathogen spores are passively transported through the xylem sap flow during transpiration (Yadeta and Thomma 2013). A similar mechanism has been reported in *Ceratocystis lukuohia* infecting ʻōhiʻa (*Metrosideros polymorpha*), indicating that members of the genus *Ceratocystis* exploit host transpiration dynamics for systemic dissemination (Hughes et al. 2020). The isolates C6ME and C8ME were identified as belonging to the ITS5 genotype, which is known for its broad host range (Tarigan et al. 2011). The high virulence of ITS5 has also been documented in jackfruit (*Artocarpus heterophyllus*) Pratama et al. (2021b) and bullet wood (*M. elengi*) (Pratama et al. 2021a). The cross-host infectivity demonstrated in this study highlights the broad ecological plasticity of *C. fimbriata*, a trait frequently observed in aggressive tropical *Ceratocystis* epidemics. The high susceptibility of *P. speciosa* and *P. americana* mirrors the rapid host-shift patterns seen in our previous research in South Sumatra and Vietnam, where *Ceratocystis* outbreaks have devastated various agroforestry

(Chi et al. 2019a; Thu et al. 2024) and *Acacia* (Chi et al. 2019b) plantations. Our findings suggest that the ITS5 haplotype in South Sumatra possesses a similarly high dissemination potential, capable of bridging the gap between managed *L. domesticum* plantations and surrounding forest ecosystems. Unlike the more localized and host-specific strains reported in some temperate regions, the South Sumatran isolates exhibit a generalized virulence profile. This lack of significant variation in isolate aggressiveness when inoculated onto *A. bubalinum* further supports the hypothesis of a highly conserved and uniformly virulent population. Consequently, the emergence of this pathogen poses a substantial biosecurity risk, as the presence of numerous alternative hosts may serve as environmental reservoirs, complicating disease management and threatening the long-term sustainability of agroforestry biodiversity in Indonesia.

The findings of this study demonstrate a significant intensification of *Ceratocystis* wilt within the surveyed orchards in Muara Enim, with disease incidence reaching 100% in specific locations. Molecular identification confirms that the representative isolates belong to the virulent ITS5 haplotype of *C. fimbriata*, which is suggestive of low detected genetic variation under the current markers at the regional scale. This genetic consistency, combined with the high pathogenicity and broad host range observed experimentally on species such as *P. speciosa* and *P. americana*, indicates a systemic threat to *L. domesticum* and the broader agroforestry biodiversity. The cross-host infectivity demonstrated here highlights the broad ecological plasticity of the pathogen, mirroring the rapid host-shift patterns documented in Vietnam, where *Ceratocystis* outbreaks have devastated various agroforestry species and acacia plantations. Our findings suggest that the ITS5 haplotype in South Sumatra possesses a high dissemination potential, capable of bridging the gap between managed plantations and surrounding forest ecosystems. This rapid progression is further exacerbated by synergistic interactions between biotic vectors, specifically squirrels and ambrosia beetles, and environmental conduits such as river systems (Suwandi et al. 2021; Muslim et al. 2022). These factors, combined with human-induced injuries from suboptimal agronomic practices, create the essential entry points required for the pathogen to initiate systemic colonization (Chi et al. 2019b).

This study confirms a critical escalation of *Ceratocystis* wilt in Muara Enim, driven by the highly aggressive ITS5 haplotype. Pathogenicity assays validate that this lineage causes systemic vascular failure and high mortality in *L. domesticum*, while exhibiting significant plasticity toward distantly related agroforestry species. To mitigate this threat, an integrated biosecurity framework is essential. Based on our findings and established protocols, effective management must prioritize the immediate removal and burning of infected trees to eliminate inoculum reservoirs (Chi et al. 2019b), avoiding new plantings in river-adjacent or infested sites to break waterborne transmission, and active monitoring of wounding agents (Lynn et al. 2025). Furthermore, rigorous tool sanitation using 75% ethanol and vector control are necessary to limit propagule dissemination. Future research should focus on wider geographic monitoring to track haplotype diversity and the screening of *L. domesticum* germplasm for genetic resistance to safeguard the long-term sustainability of polyculture systems in South Sumatra.

In conclusion, this study demonstrates that *Ceratocystis* wilt in *L. domesticum* has reached epidemic levels across eight production centers in Muara Enim, South Sumatra, with incidence and intensity rising sharply from 2023 to 2025 and some villages reaching 100%. Field symptom progression was rapid, leading to tree death within 2-3 months, and was strongly associated with wounding from pruning and squirrel feeding, as well as boring by ambrosia and mango bark beetles that likely enhance pathogen entry and dispersal. Carrot baiting reliably recovered *Ceratocystis* isolates, which showed uniform cultural and morphological traits consistent with the *C. fimbriata* complex. ITS and β-tubulin sequencing placed all representative isolates in the globally widespread ITS5 haplotype, indicating low detected genetic variation in the outbreak population. Koch's postulates confirmed high virulence and broad host infectivity, underscoring serious risks to mixed agroforestry systems. Immediate sanitation, inoculum removal, vector and wound management, and expanded surveillance are essential to curb further losses.

ACKNOWLEDGEMENTS

This research was funded by Universitas Sriwijaya, Indonesia (Rector's Decree No. 0459/E5/PG.02.00/2024, dated 17 September 2024). The author also wishes to thank the *duku* farmers in South Sumatra and the *duku* thesis team, students of the Plant Protection Department, Faculty of Agriculture, Universitas Sriwijaya, who participated in this research, for their support and assistance in plant sampling and data collection.

REFERENCES

Ahmad MF, Zahari R, Mohtar M, Wan-Muhammad-Azrul WA, Hishamuddin MS, Samsudin NIP, Hassan A, Terhem R. 2022. Diversity of endophytic fungi isolated from different plant parts of *Acacia mangium,* and antagonistic activity against *Ceratocystis fimbriata*, a causal agent of *Ceratocystis* wilt disease of *A. mangium* in Malaysia. Front Microbiol 13: 887880. https://doi.org/10.3389/fmicb.2022.887880.

Atmojo YK, Irwan SNR, Rogomulyo R. 2018. Selection of alternative fruit trees for reforestation based on plant characteristics and land suitability in the Bantul Regional Government Office area, Manding, Yogyakarta. Vegetalika 7 (4): 74-88. https://doi.org/10.22146/veg.41176. [Indonesian]

Carluccio G, Greco D, Sabella E, Vergine M, De Bellis L, Luvisi A. 2023. Xylem embolism and pathogens: Can the vessel anatomy of woody plants contribute to *X. fastidiosa* resistance? Pathogens 12 (6): 825. https://doi.org/10.3390/pathogens12060825.

Chi NM, Nhung NP, Trang TT, Thu PQ, Hinh TX, Nam NV, Quang DN, Dell B. 2019a. First report of wilt disease in *Dalbergia tonkinensis* caused by *Ceratocystis manginecans.* Australas Plant Pathol 48: 439-445. https://doi.org/10.1007/s13313-019-00643-1.

Chi NM, Thu PQ, Hinh TX, Dell B. 2019b. Management of *Ceratocystis manginecans* in plantations of *Acacia* through optimal pruning and site selection. Australas Plant Pathol 48: 343-350. https://doi.org/10.1007/s13313-019-00635-1.

Fernandes BV, Zanuncio AJV, Furtado EL, Andrade HB. 2014. Damage and loss due to *Ceratocystis fimbriata* in *Eucalyptus* wood for charcoal production. BioResources 9 (3): 5473-5479. https://doi.org/10.13140/2.1.3142.4643.

Hall TA. 1999. BioEdit: A user-friendly biological sequence alignment Editor and analysis program for Windows 95/98/NT. Nucleic Acids Symp Ser 41: 95-98.

Harrington TC, Kazmi MR, Al-Sadi AM, Ismail SI. 2014. Intraspecific and intragenomic variability of ITS rDNA sequences reveals taxonomic problems in *Ceratocystis fimbriata* sensu stricto. Mycologia 106 (2): 224-242. https://doi.org/10.3852/13-189.

Hughes MA, Juzwik J, Harrington TC, Keith LM. 2020. Pathogenicity, symptom development, and colonization of *Metrosideros polymorpha* by *Ceratocystis lukuohia*. Plant Dis 104 (8): 2233-2241. https://doi.org/10.1094/pdis-09-19-1905-re.

Jimu L, Wingfield MJ, Mwenje E, Roux J. 2015. Diseases on *Eucalyptus* species in Zimbabwean plantations and woodlots. South For J For Sci 77 (3): 221-230. https://doi.org/10.2989/20702620.2014.1001682.

Li Q, Harrington TC, McNew D, Li J, Huang Q, Somasekhara YM, Alfenas AC. 2016. Genetic bottlenecks for two populations of *Ceratocystis fimbriata* on sweet potato and pomegranate in China. Plant Dis 100 (11): 2266-2274. https://doi.org/10.1094/pdis-03-16-0409-re.

Lynn KMT, Wingfield MJ, Tarigan M, Durán A, Santos SA, Nel WJ, Barnes I. 2025. Investigating bark, ambrosia and nitidulid beetle (Coleoptera: Scolytinae and Nitidulidae) communities and their potential role in the movement of *Ceratocystis manginecans* in commercial forestry plantations in Riau, Indonesia. Agric For Entomol 27 (4): 707-722. https://doi.org/10.1111/afe.12698.

Muslim A, Pratama R, Suwandi S, Hamidson H. 2022. Diseases severity, genetic variation, and pathogenicity of Ceratocystis Wilt on *Lansium domesticum* in South Sumatra, Indonesia. Plant Pathol J 38 (2): 131-145. https://doi.org/10.5423/ppj.oa.12.2021.0182.

Muslim A, Suwandi S, Pratama R, Gunawan B. 2025. *Ceratocystis fimbriata* causing canker and wilt disease on West Indian mahogany trees in Indonesia. J Plant Dis Prot 132: 12. https://doi.org/10.1007/s41348-024-00995-x.

Oliveira LSS, Harrington TC, Ferreira MA, Damacena MB, Al-Sadi AM, Al-Mahmooli IHS, Alfenas AC. 2015. Species or genotypes? Reassessment of four recently described species of the *Ceratocystis* wilt pathogen, *Ceratocystis fimbriata*, on *Mangifera indica*. Phytopathology 105 (9): 1229-1244. https://doi.org/10.1094/phyto-03-15-0065-r.

Pratama R, Muslim A, Damiri N, Hamidson H, Suwandi, Amelia RP. 2026. *Ceratocystis fimbriata* causing wilt and sudden death on *Acacia mangium* in South Sumatera. Curr Appl Sci Technol 26 (1): e0265486. https://doi.org/10.55003/cast.2025.265486.

Pratama R, Muslim A, Suwandi S, Damiri N, Soleha S. 2021a. First report of bullet wood (*Mimusops elengi*) sudden decline disease by Ceratocystis in Indonesia. Biodiversitas 22 (5): 2636-2645. https://doi.org/10.13057/biodiv/d220522.

Pratama R, Muslim A, Suwandi S, Damiri N, Soleha S. 2021b. Jackfruit (*Artocarpus heterophyllus*), a new host plant of *Ceratocystis* wilt in South Sumatra, Indonesia. Australas Plant Dis Notes 16: 24. https://doi.org/10.1007/s13314-021-00435-x.

Pratama R, Suwandi S, Muslim A, Mulawarman. 2025. Diversity of *Ceratocystis fimbriata* causing canker and wilt disease on *Cupressus sempervirens* (Italian cypress) in Indonesia. Biodiversitas 26 (1): 278-287. https://doi.org/10.13057/biodiv/d260128.

Rahayu S, Nurjanto HH, Pratama RG. 2015. Characteristics of fungi *Ceratocystis* sp. causing stem rot disease in *Acacia decurrens* and its disease status in Mount Merapi National Park, Yogyakarta. J Ilmu Kehutanan 9 (2): 94-104. https://doi.org/10.22146/jik.10193. [Indonesian]

Roy K, Ewing CP, Hughes MA, Keith L, Bennett GM. 2018. Presence and viability of *Ceratocystis lukuohia* in ambrosia beetle frass from Rapid ʻŌhiʻa death-affected *Metrosideros polymorpha* trees on Hawaiʻi Island. Forest Pathol 49 (1): e12476. https://doi.org/10.1111/efp.12476.

Roy K, Jaenecke KA, Peck RW. 2020. Ambrosia beetle (Coleoptera: Curculionidae) communities and frass production in ʼŌhiʻa (Myrtales: Myrtaceae) infected with *Ceratocystis* (Microascales: Ceratocystidaceae) fungi responsible for rapid ʼŌhiʻa death. Environ Entomol 49 (6): 1345-1354. https://doi.org/10.1093/ee/nvaa108.

Safety AIK, Sjarkowi F, Bidarti A. 2024. The impact of farming land function of farming to housing towards sustainable food availability in Empelas Pills Village Muara Enim district. Oryza: Jurnal Agribisnis dan Pertanian Berkelanjutan 9 (2): 17-28. https://doi.org/10.56071/oryza.v9i2.928. [Indonesian]

Safitri A, Harvianti Y, Pratama R. 2025. First report of *Ceratocystis manginecans* causing wilt and sudden death in *Bouea macrophylla* (Plum mango) in Indonesia. New Dis Rep 52 (2): e70095. https://doi.org/10.1002/ndr2.70095.

Sulistyantara B, Damayanti R, Manningtyas T, Fatimah IS, Pamungkas AA, Ardhana FA. 2024. Implementation of grafting techniques to increase productivity and sustainability of local *duku* fruit plants (*Lansium domesticum*) in Arisan Buntal Village, South Sumatra. Agrokreatif 10 (3): 281-288. https://doi.org/10.29244/agrokreatif.10.3.281-288. [Indonesian]

Suwandi S, Irsan C, Hamidson H, Umayah A, Asriyani KD. 2021. Identification and characterization of *Ceratocystis fimbriata* causing lethal wilt on the *Lansium* tree in Indonesia. Plant Pathol J 37 (2): 124-136. https://doi.org/10.5423/ppj.oa.08.2020.0147.

Syazwan SA, Mohd-Farid A, Wan-Muhd-Azrul W-A, Syahmi HM, Zaki AM, Ong SP, Mohamed R. 2021. Survey, identification, and pathogenicity of *Ceratocystis fimbriata* complex associated with wilt disease on *Acacia mangium* in Malaysia. Forests 12 (12): 1782. https://doi.org/10.3390/f12121782.

Tarigan M, Roux J, Van Wyk M, Tjahjono B, Wingfield MJ. 2011. A new wilt and die-back disease of *Acacia mangium* associated with *Ceratocystis manginecans* and *C. acaciivora* sp. *nov*. in Indonesia. S Afr J Bot 77 (2): 292-304. https://doi.org/10.1016/j.sajb.2010.08.006.

Thu PQ, Duc DT, Chi NM, Anh DTK, Thuy PTT, Loi VV, Loan NT, Hang NTM, Dell B. 2024. *Ceratocystis fimbriata sensu lato* causes canker and wilt diseases of urban park trees in Hanoi, Vietnam. Indian Phytopathol 77: 397-405. https://doi.org/10.1007/s42360-024-00734-0.

Trang TT, Eyles A, Davies N, Glen M, Ratkowsky D, Mohammed C. 2018. Screening for host responses in *Acacia* to a canker and wilt pathogen, *Ceratocystis manginecans*. Forest Pathol 48 (1): e12390. https://doi.org/10.1111/efp.12390.

White TJ, Bruns T, Lee S, Taylor JW. 1990. Amplification and direct sequencing of fungal ribosomal RNA genes for phylogenetics. In: Innis MA, Gelfand DH, Sninsky JJ, White TJ (eds). PCR Protocols: A Guide to Methods and Applications, Academic Press, New York. http://dx.doi.org/10.1016/B978-0-12-372180-8.50042-1.

Xu KC, Zhang RQ, Li J, Bai YH, Yang XD, Sun YX, Huang Q. 2019. *Camellia sinensis*, a new host plant of *Ceratocystis fimbriata* from China. Plant Dis 103 (10) 2670-2679. https://doi.org/10.1094/pdis-04-19-0802-pdn.

Yadeta KA, Thomma BPHJ. 2013. The xylem as battleground for plant hosts and vascular wilt pathogens. Front Plant Sci 4: 97. https://doi.org/10.3389/fpls.2013.00097.

Zhu Y, Lujan P, Dura S, Steiner R, Zhang J, Sanogo S. 2019. Etiology of Alternaria leaf spot of cotton in Southern New Mexico. Plant Dis 103: 1595-1604. https://doi.org/10.1094/pdis-08-18-1350-re.